UNIVERSITY OF SASKATCHEWAN
100 YEARS Engage·Enlighten·Explore

An Automated Gauge for Acoustically Determining Snow Water Equivalent

N.J. Kinar[1] and J.W. Pomeroy[2]
1. Centre for Hydrology, University of Saskatchewan, Saskatoon, Saskatchewan, Canada. S7N 5C8 (n.kinar@usask.ca)
2. Centre for Hydrology, University of Saskatchewan, Saskatoon, Saskatchewan, Canada. S7N 5C8 (john.pomeroy@usask.ca)

CENTRE FOR HYDROLOGY

BACKGROUND

Measurements of Snow Water Equivalent (SWE) generally involve invasive devices that modify the snowpack. To estimate SWE in an operational context, a gravimetric sample is taken to determine the density of snow, and snow depth is found using a ruler (Figure 1).

Figure 1. Snow surveying in Wolf Creek Research Basin, Yukon

- Despite the fact that such instruments enjoy widespread use, snow surveying for the determination of SWE is a primitive, laborious task that is time-consuming, expensive, and prone to human error. The equipment used has not evolved significantly for almost one century.
- Measurements made by devices such as Frequency-Modulated Continuous-Wave (FMCW) radar have shown utility in estimating snow depth or density, but not both.
- Previous research conducted at the Centre for Hydrology demonstrated the possibility of determining SWE by the use of a frequency-swept acoustic impulse.
- As an extension of this research, custom electronic circuitry was designed to create a portable gauge suitable for determining SWE by the theory and techniques outlined by Kinar and Pomeroy (2007).

SYSTEM ARCHITECTURE

- The system is comprised of a number of sub-systems (Figure 2) which are indicative of six design goals (Figure 3):

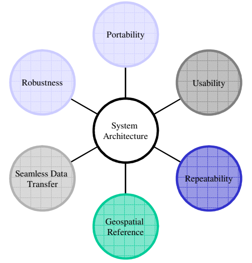

Figure 3. Design goals influencing system architecture

The finished gauge is depicted in Figure 4 and the following description refers to components marked on the diagram:

- A) **Crush resistant enclosure** that shields the 'system' of custom-designed circuit boards.
- B) **Transducer** (loudspeaker) capable of producing an audible sound wave in the frequency range of 20 Hz to 20 kHz.
- C) **Microphone**, which detects the sound pressure wave.
- D) **Thermometer**, which determines air temperature.
- E) **Pistol grip**, which allows the user to hold the device.
- F) **Pushbutton switch**, used to turn on the system.
- G) **LCD displays**, to provide system operation information.
- H) **Light-Emitting Diodes**, to show user selection choices.
- I) **Keypad**, to provide user feedback.

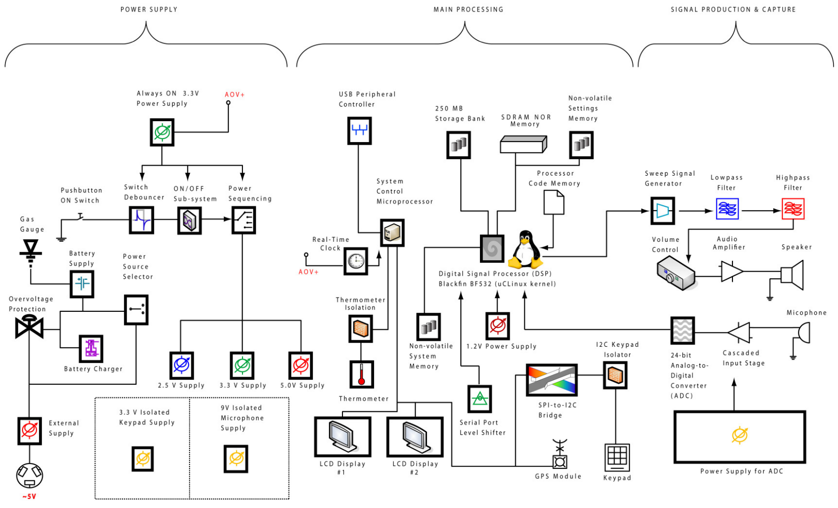

Figure 2. Block diagram of the system

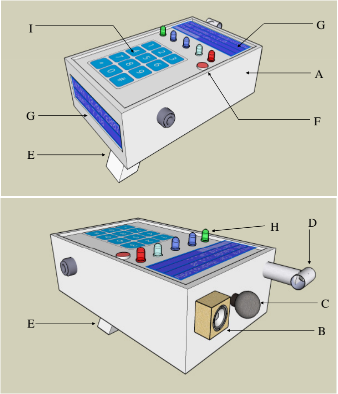

Figure 4. Schematic diagram of the system

Signal Processing

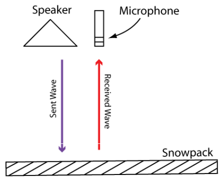

Figure 5. Schematic diagram of the measurement system

- An acoustic frequency-swept wave is sent into the snowpack from the speaker.
- The wave reflected from the snowpack is captured by the microphone (Figure 5), digitized by the Analog-to-Digital converter, and the wave is then stored as a numerical sequence in the memory of the gauge (Figure 2).
- Due to the close proximity of the loudspeaker to the microphone, a sound wave will travel from the speaker directly to the microphone (Figure 6A). This must be removed before other signal processing occurs (Figure 6B):

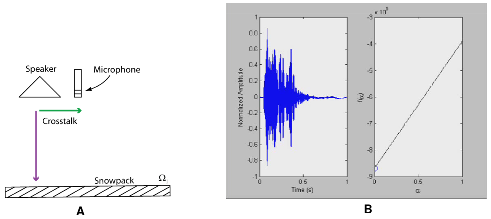

A B

Figure 6. Diagram showing crosstalk between the speaker and the microphone

- The objective is to minimize the coupling coefficient:

$$\min_{\alpha}\left[\sum_{i=1}^{N}\frac{\left(s_1'[t]-\alpha s_1'[t]\right)^2}{\left(s_1'[t]\right)^2+\sigma^2}\right]$$

$\alpha =$ coupling coefficient
$\sigma =$ noise level of signal
$s[t] =$ original wave
$s'[t] =$ reflected wave

- In the same manner as Frequency-Modulated Continuous-Wave (FMCW) Radar, the original and reflected waves are homodyned by multiplication in the time domain.
- The difference beat frequencies are proportional to the distance to a layer in the snowpack. Reflections occur due to changes in acoustic impedance (Figure 7A).

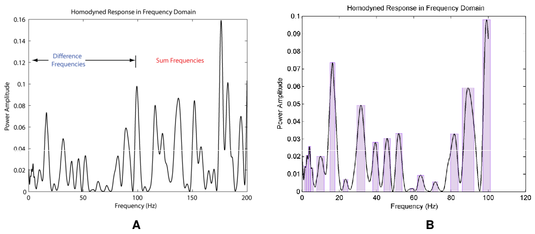

A B

Figure 7. Diagram showing the homodyning process in the frequency domain

- Each peak in the homodyned response is coincident with a reflection from a layer in the snowpack. Automatic peak detection is performed by an algorithm that examines the smoothed first derivative for turning points and performs least-squares curve fitting to determine the top of each peak (Figure 7B).

- Previous work conducted by the Centre for Hydrology utilized a convolution model to determine reflection coefficients of snowpack layers by division in the frequency domain. This was prone to problems such as noise and unstable filter kernels. It is possible to bypass this step by changing the theory.

- This procedure utilizes a layer-stripping approach where the reflection coefficients of upper layers are used to calculate the reflection coefficients of layers situated at greater depth in the snowpack
- Determining the reflection coefficients involves Newton iteration:

$$P_0(t)=\sum_{i=1}^{n}0.5A_i\cos\left(2\pi k t_i\right)t$$

$$\boxed{\Gamma_n\prod_{i=1}^{n}\left(1-\Gamma_i\right)^2-\left(A_n/\pi\left(1-\Gamma_n\right)\right)=0}$$

$P_o(t) =$ Signal power output
$A_i =$ Amplitude of a peak
$k =$ Angular wavenumber
$\Gamma_n =$ reflection coefficient

- The reflection coefficients are transformed from spherical to planar by a Hankel Transform of the Sommerfeld Integral.
- We stabilize the transform used in our previous research by using an approximation and "windowing" the integrand by multiplication with a masking function. This allows for integration to occur in the vicinity of stationary phase points which contribute non-negligible area to the integration.

$\exp\left[i\cdot A\chi^2\right]$ $\exp\left[i\cdot A\chi^2\right]\times\exp\left[-B\chi^n\right]$

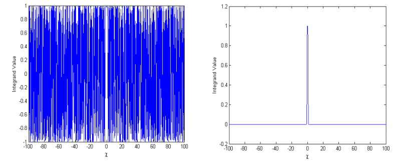

Figure 8. Demonstration of stabilizing the transform.

- Because the wave sent into the snowpack is frequency-swept, the angular wavenumber k used in the transform changes over the time of the sweep.
- Coherent reflection from the snow surface is modeled by generating a plasma fractal and then using this as an estimate of snow surface roughness (Figure 9).
- The Rayleigh parameter is then averaged by integrating over the bandwidth of the frequency sweep.

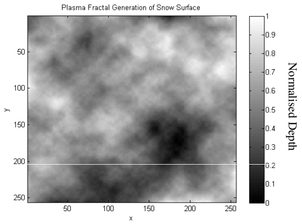

Figure 9. Generation of plasma fractal from the snow surface.

Locations and Methodology

- The automated gauge was tested during April 2007 at two field locations (forested and shrub tundra) in the Wolf Creek Research Basin. An on-board GPS module recorded the positions of the sites (Figure 10).
- Wolf Creek is a 195 km^2 glaciated sub-arctic basin situated near Whitehorse, Yukon. It is characterized by boreal forest, shrub tundra and sparse alpine tundra.
- The snow found at these sites was partly wetted and heavily wind-crusted, and the snowpack was underlain with twigs, branches, and buried grasses, shrubs and tree branches.

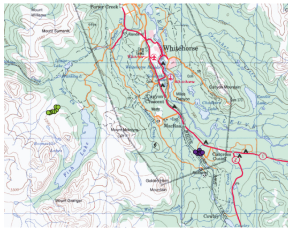

Figure 10. Map showing the GPS locations of the points 🟢 Represents Shrub Tundra Site
🟣 Represents Forest Site

Results

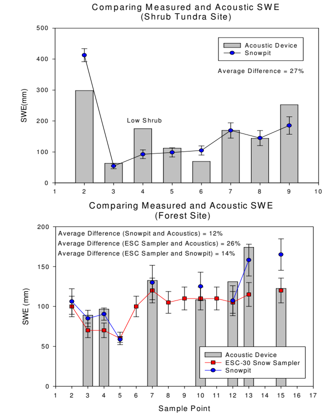

Figure 5. Results from the Granger Basin and Forest Site

- The results show average difference of 27% between the measured and acoustic estimates of SWE.
- Acoustic estimates of SWE are closer to snowpit gravimetric measurements than are measurements made by an ESC30 snow density sampler and ruler.
- Vegetation sometimes caused the acoustic predictions of SWE to be overestimated due to scattering of the sound wave.
- Attenuation of the sound wave by heavily crusted deep snow resulted in an underestimation of SWE

Conclusions

- SWE can be determined by a frequency-swept wave with a frequency in the audible (20 Hz to 20 kHz) range.
- The acoustic method has similar errors to gravimetric sampling for many snowpacks.
- This method has the potential to determine SWE without disrupting the snowpack.
- The acoustic method has been successfully tested in an operational context at two sub-Arctic sites.
- Buried vegetation and extremely deep, dense snowpacks present measurement problems for the device as currently configured.

Acknowledgements

- An NSERC PGS-M Scholarship (NJK), the Improved Processes and Parameterisation for Prediction (IP3) Network of CFCAS, and the Canada Research Chairs Program (JWP).

- Maxim/Dallas Integrated Circuits for sending a development kit which allowed for the testing of signal processing algorithms